Partial weight suspension: a novel murine model for investigating adaptation to reduced musculoskeletal loading

Erika B Wagner [1,2,✉], Nicholas P Granzella [2], Hiroaki Saito [3], Dava J Newman [2], Laurence R Young [2], Mary L Bouxsein [4]

Author information   Article notes   Copyright and License information
PMCID: PMC3774184   PMID: 20522735

Abstract

We developed a new model of hypodynamic loading to support mice in chronic conditions of partial weight bearing, enabling simulations of reduced gravity environments and related clinical conditions. The novel hardware allows for reduced loading between 10 and 80% of normal body weight on all four limbs and enables characteristic quadrupedal locomotion. Ten-week-old female BALB/cByJ mice were supported for 21 days under Mars-analog suspension (38% weight bearing) and compared with age-matched and jacketed (100% weight bearing) controls. After an initial adaptation, weight gain did not differ between groups, suggesting low levels of animal stress. Relative to age-matched controls, mice exposed to Mars-analog loading had significantly lower muscle mass (-23% gastrocnemius wet mass, $P < 0.0001$); trabecular and cortical bone morphology (i.e., trabecular bone volume: -24% at the distal femur, and cortical thickness: -11% at the femoral midshaft, both $P < 0.001$); and biomechanical properties of the femoral midshaft (i.e., -27% ultimate moment, $P < 0.001$). Bone formation indexes were decreased compared with age-matched full-weight-bearing mice, whereas resorption parameters were largely unchanged. Singly housed, full-weight-bearing controls with forelimb jackets were largely similar to age-matched, group-housed controls, although a few variables differed and warrant further investigation. Altogether, these data provide strong rationale for use of our new model of partial weight

bearing to further explore the musculoskeletal response to reduced loading environments.

MUSCULOSKELETAL DECONDITIONING associated with spaceflight has been noted since the early days of the Gemini program. Despite rigorous exercise protocols and other countermeasures, negative calcium balance (~0.5%/mo) and bone loss in weight-bearing bones (1.0–2.7%/mo) are still the hallmarks of flight (12–15, 29). Although the mechanisms of disuse-induced bone loss and age-related bone loss are not identical, a 20% decline in femoral neck bone mineral density during a single year of spaceflight corresponds to 30 yr of age-related bone loss in a postmenopausal woman, bringing with it a significant increase in fracture risk (16). Furthermore, subject-specific finite-element analyses indicate that femoral bone strength declines by 2%/mo during spaceflight, with some astronauts exhibiting reductions in proximal femoral strength that are comparable to estimated lifetime losses in bone strength associated with aging (11).

Whereas human spaceflight over the last 30 yr has been confined exclusively to low Earth orbit, and largely to flights of less than 6 mo, exploration goals once again reach beyond the Van Allen belts. Although the physiological effects of weightlessness are well described, the effects of chronic partial weight bearing, such as expected on the moon (16% of Earth's gravity) and Mars (38% of Earth's gravity), have yet to be quantified. In these environments, the risks of musculoskeletal atrophy and accompanying orthopedic injury are uncertain, and methods to further investigate adaptations to partial weight bearing are needed.

Based on the paradigm that mechanical loading provides the primary stimulus for skeletal maintenance (4, 10, 24), it is likely that partial weight bearing will provide some prophylaxis against the deconditioning seen in conditions of full disuse. But how do adaptive processes scale with changes in gravitational loading? Does a given decrease in gravitational acceleration lead to a proportionate decrease in bone and muscle mass, or is this response curve nonlinear? The answers to these questions are important, not only for aerospace physiology, but also for a better understanding of the effects of reduced weight bearing associated with clinical conditions and diseases.

Accordingly, the objectives of this study were to develop a new rodent model of partial weight suspension (PWS) to explore these musculoskeletal effects of chronically reduced weight bearing and to conduct the first study of musculoskeletal adaptation to Mars gravity levels. We hypothesized that musculoskeletal adaptation to partial weight bearing would replicate the key features of adaptation to full unloading, including reduced bone formation rate, muscle mass, bone mass, and bone strength.

MATERIALS AND METHODS

We first describe the development of the PWS system and then detail an in vivo study with mice exposed to Mars-analog loading.

Description of PWS system.

The PWS system draws on design elements developed for human research in partial weight-bearing locomotion, coupling them with lessons learned over 3 decades of rodent suspension (2, 18, 22). Developed for the National Aeronautics and Space Administration (NASA) in 1979, classic hindlimb or tail suspension utilizes tail traction and hindquarter elevation to fully unload the animal's rear limbs, while the forelimbs remain weight bearing and support locomotion. Bone loss and muscle atrophy accompany this disuse, providing a good model for studying the effects of, and countermeasures to, spaceflight and other disuse. However, the model is not readily extensible to loading conditions between normal and full unloading.

The PWS system was designed, and verified in testing, to *1*) support mice in partial weight-bearing quadrupedal loading for periods of at least 3 wk; *2*) be tunable to within ±5% of a desired hypodynamic stimulus between 10 and 80% weight bearing; *3*) provide an environment that minimizes stress to the animals, as measured by body mass changes; *4*) support movement, cleaning, and feeding; and *5*) allow for full recovery to facilitate reloading studies.

All experimental protocols were approved by the Massachusetts Institute of Technology Animal Care and Use Committee. Animals were singly housed in specially developed habitats derived from designs of NASA Ames Research Center and Cornell University (18). The living volumes were 12-in. polycarbonate cubes, with wooden feet supporting the corners and removable perforated floors that passively minimized waste buildup. Sitting atop the cages, an aluminum channel provided a rigid base for suspension hardware (Fig. 1*A*). A steel rod supported a small nylon wheel and low-friction bearing to provide linear freedom of motion for the suspended animals.

Fig. 1.
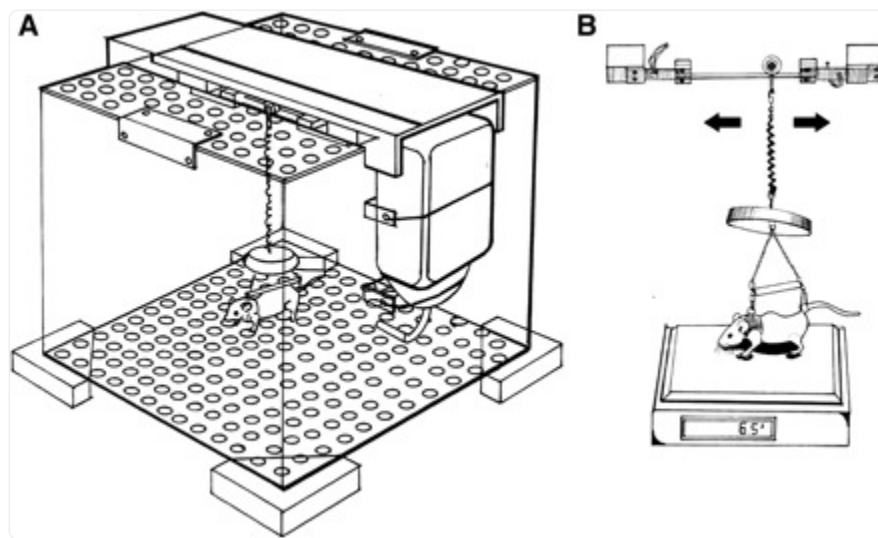
A: Partial Weight Suspension habitat with polycarbonate walls, perforated PVC floor and lid, and aluminum channel supporting suspension hardware. Note that holes in this drawing are oversized. Actual openings are 4.8 mm in diameter and allow for passive passage of waste without risk of injury to the animals. *B*: system for measuring effective body mass. Animals were suspended above a scale, and spring tension was adjusted to provide the desired level of partial weight bearing. [Image credit: Shaun Modi]

In contrast to previous models (25), we opted for a quadrupedal suspension design to help preserve normal gait characteristics and loading patterns. A full-body suspension design was developed around the traditional Morey-Holton tail suspension model and previous whole body harness models (19, 25). A "second-skin" bandage of Tegaderm or SteriStrip (3M, St. Paul, MN) was loosely wrapped at the base of the tail to prevent irritation, and a small piece of athletic tape secured the tail to the harness. The forelimbs were supported by a flexible, breathable "jacket" of athletic tape and soft moleskin, secured by Velcro under isoflurane anesthesia. Several pilot studies resulted in the optimization of the jacket design, allowing the jacketed mice to demonstrate feeding, grooming, sleeping, exploring, and other appropriate daily activities. As seen in Fig. 1*B*, the harness and tail wrap were connected by an adjustable bead chain and spaced by a hollow metal rod to distribute loading.

A previously published system that supported partial weight bearing on the forelimbs with unloaded hindlimbs relied on a complex active feedback system to provide frequency-tuned loading (25). We opted instead to focus on adjusting peak loading levels with minimum complexity. Thus we implemented a passive suspension design using a low-modulus

plastic-coated spring ($k \approx 1.6$ N/m; S0101 coil cord, Statico, San Carlos, CA). Twisting the spring through its support engaged a variable number of coils, N, thereby changing the spring constant proportional to $1/N$. Small swivels prevented spring bind-up, and a plastic lid secured above the animal inhibited climbing. Total mass of the suspension element was 14 g, which was fully supported under static conditions and did not contribute to the standing mass of the animal.

Daily weighing of suspended animals quantified the static loads experienced during quiet standing. True body masses were first obtained by briefly hanging the animal on a specially designed rig positioned over a scale, so as to avoid full weight bearing (18). Titrated weight bearing, expressed throughout as effective body mass, was then measured with the animal standing in quadrupedal PWS on the same scale (Fig. 1B). Adjustments to spring tension were made as necessary to accommodate changes in body mass and spring stiffness.

Ground reaction force measurement.

To quantify the dynamic loading environment of PWS, a high-precision three-axis force plate (HE-6x6-1 AccuSway Force Plate, AMTI Measurements, Watertown, MA) was used to measure ground reaction forces (GRF) during active locomotion. A plywood platform was built over the plate to provide a level walking surface, with a 2-cm-wide strip of plywood atop the force plate as a local load sensor, as described by Zumwalt et al. (33). The platform was covered with cloth tape to improve traction, and mice locomoted freely over the surface. GRFs were collected in three orthogonal directions: X (nose to tail), Y (mediolateral), and Z (vertical). Signals were filtered with a two-pole, low-pass Butterworth filter with a corner frequency of 25 Hz (MATLAB filter routine, The Mathworks, Natick, MA). Peak forces were identified in all three directions. The rate of force onset was estimated as the slope of the initial portion of the GRF rise. Stance duration and area under the force curve were also calculated.

Trials were conducted with and without a forelimb vest, and under PWS at 16, 38, and/or 60% weight bearing. Traces were selected for analysis whenever a single forelimb made unobstructed contact with the local load sensor strip. In most cases, this first forelimb footfall was immediately followed by the ipsilateral hindlimb. All evaluated impacts were confirmed with video footage. Data were gathered from a single female mouse (10 wk old, BALB/cByJ) for internal consistency and includes pairs of footfalls from normal gait ($n = 4$), jacketed gait ($n = 5$), and suspension at 60% ($n = 5$), 38% (Mars, $n = 4$), and 16% (Lunar, $n = 11$ forelimb, 3 hindlimb) weight bearing.

Design of Mars-analog weight-bearing study.

Ten-week-old female nulliparous BALB/cByJ mice were obtained from Jackson Laboratories (Bar Harbor, ME). This age was chosen to take advantage of the plateau in longitudinal femoral growth, which is more representative of the adult human skeleton, and a near maximum in trabecular bone volume (5, 6), which improves the likelihood of

visualizing changes in this compartment.

Animals were randomly assigned to four groups: Baseline (killed at start, $n = 8$), Age-matched (killed at end, $n = 21$ to provide additional statistical power), Mars (38% weight bearing, $n = 10$), and Jacket controls (100% weight bearing, $n = 13$). Baseline and Age groups were group-housed in standard laboratory vivarium caging with ad libitum access to both food and water. Mars animals were singly housed, harnessed, and suspended at 38% weight bearing for 21 days. Jacket control animals were similarly harnessed and singly housed in experimental cages, but remained fully weight bearing for the 21-day experiment. Before the start of the experiment, Mars and Jacket mice underwent a 2-day period of adaptation to the forelimb harnesses. Food and water access were provided ad libitum in Mars, Age, and Baseline groups, whereas Jacket mice were pair-fed, according to the previous day's average of the Mars cohort. Daily care, weighing, and adjustment of spring tension were provided to all animals as described above. One Mars mouse was removed from the study due to self-inflicted tail injury. Two Jacket animals were removed due to excessive weight loss caused by failure to adapt to the harnesses. Four additional mice (1 Age, 3 Jacket) were removed due to complications arising from a prestudy blood draw.

Intraperitoneal injections of calcein (0.05 ml, 12 mg calcein/ml of 2% saline-bicarbonate solution, ∼30 mg/kg) were given at 10 and 2 days before death to label newly forming bone. Following death by carbon dioxide inhalation, the gastrocnemius muscles were weighed. Femurs, tibiae, and humerii were harvested bilaterally from all study animals. Left side bones were prepared for imaging and biomechanical testing in gauze soaked in normal saline (0.9%), then stored at −20°C. Right side bones were prepared for histology in 10% neutral buffered formalin at 4°C for 48–72 h, then transferred to 70% ethanol, and returned to refrigeration.

Bone microarchitecture.

Trabecular and cortical bone microarchitecture were assessed using high-resolution microcomputed tomography (μCT40; Scanco Medical, Basserdorf, Switzerland), as previously described (5). Briefly, the distal femoral metaphysis and femoral midshaft were scanned using a 12-μm isotropic voxel size. Morphometric parameters were computed using a direct three-dimensional approach that does not rely on any assumptions about the underlying structure. For the cancellous bone region, we assessed bone volume fraction [bone volume per total volume (BV/TV), %], trabecular thickness (μm), trabecular separation (μm), trabecular number (mm^{-1}), connectivity density (mm^{-3}), and structure model index. For the cortical regions at the distal femoral metaphysis and femoral midshaft, we measured the total cross-sectional area, cortical bone area (BA), medullary area (all mm^2), and cortical thickness (Ct.Th; μm). The maximum, minimum, and polar (all mm^4) moments of inertia were also measured at the femoral midshaft.

Biomechanical assessment.

Following µCT scanning, the strength of the femoral midshaft was assessed by 3-point bending. Specimens were thawed to room temperature in physiological saline to ensure adequate hydration, then placed posterior surface downward on a 6-mm span. A low-force mechanical testing system (MTS Bionix 200, with 100 N load cell, MTS Systems, Eden Prairie, MN) was used to apply a flexion moment to the midpoint of the anterior diaphysis. A preload of 1–2 N was applied, followed by a constant displacement rate of 0.03 mm/s until failure. Force-displacement data were acquired at 100 Hz and used to determine structural properties (moment at yield, ultimate moment, bending stiffness, and postyield work). Bending rigidity for each specimen was normalized by the minimum moment of inertia, as measured on the µCT scans, to derive an estimated elastic modulus. Three specimens (one Age and two Mars) were removed due to technical errors during the mechanical testing.

Histomorphometry.

Following µCT, the five tibiae in each group nearest to the median value for trabecular bone volume fraction were selected for histomorphometry, then processed using previously described methods (26). Un-decalcified thin sections (4 µm) were prepared and stained with toluidine blue or left unstained. A standard histomorphometric analysis of the proximal tibial metaphysis was performed (OsteoMeasure analysis system, OsteoMetrics, Decatur, GA) in a 1.28-mm^2 area starting 0.3 mm distal from the growth plate. Histomorphometry methods, variables, and nomenclature conform to those recommended by the American Society for Bone and Mineral Research (23).

Data analysis.

To examine the effect of aging during the study, we compared Age mice to Baseline mice using unpaired t-tests. To examine the differences between Age, Jacket, and Mars groups, we utilized an ANOVA with Fisher's paired least significant difference for post hoc comparisons. Differences were considered significant when $P < 0.05$.

RESULTS

GRFs.

For each of the 21 days of the study, static values of effective body mass were set within 1 g of the desired weight-bearing level (mean error = −4.1 ± 1.0% true body mass). Average drift overnight was 0.5 g (2.5 ± 4.9% true body mass). Static weight bearing at the beginning and end of each day remained within 5% of target levels on 77% of study days, deviating >10% from desired weight bearing on <2% of all study days.

During locomotion, peak dynamic GRFs in the vertical direction were reduced ∼25 and 14% in the forelimbs and hindlimbs, respectively, by application of the jacket, suggesting a relative unweighting of the forelimbs due to the

restrictions of the forelimb vest. Compared with full weight bearing, Mars weight bearing reduced the mean peak vertical GRF at self-selected walking speeds by 64% in the forelimbs and 85% in the hindlimbs, while Lunar weight bearing reduced mean peak vertical GRF at self-selected walking speeds by 75% in the forelimbs and 85% in the hindlimbs ($P < 0.001$ for all relative to full weight bearing, Fig. 2, Table 1).

Fig. 2.
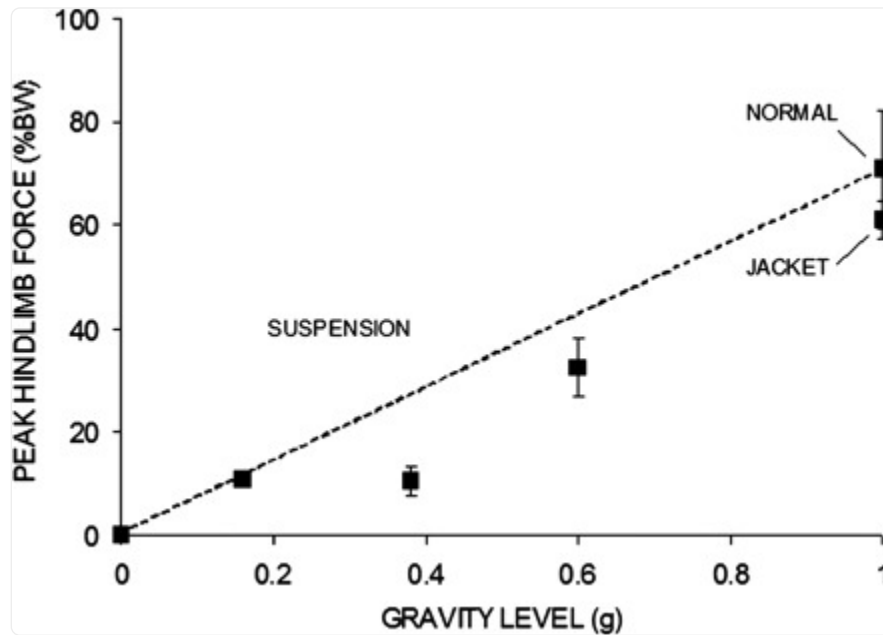
Open in a new tab

Relationship between peak vertical ground reaction forces and simulated gravity level, where 1 g represents full weight bearing. Data come from repeated trials in the same animal. Dotted trend line represents a hypothesized linear relationship between the two variables. BW, body weight. Error bars represent ± SD.

Table 1.

Ground reaction force data from AccuSway platform

	Normal	Jacket	60%	Mars	Lunar
n	4	5	5	4	11 forelimb, 3 hindlimb
Peak IGRF$_z$|, %BW					
Forelimb	78.85 ± 13.66	59.48 ± 12.93[*]	41.93 ± 8.45[*]	28.63 ± 2.92[*]	20.09 ± 5.06[*]
Hindlimb	70.93 ± 11.53	61.10 ± 3.65	32.43 ± 5.80[*]	10.44 ± 2.99[*]	10.92 ± 1.21[*]
Peak |GRF$_x$|, %BW					
Forelimb	18.25 ± 14.11	11.23 ± 7.87	15.06 ± 4.90	10.04 ± 2.72	6.21 ± 2.67[*]
Hindlimb	16.42 ± 7.42	13.65 ± 7.92	15.57 ± 6.65	5.00 ± 3.80[*]	3.96 ± 3.75[*]
Peak |GRF$_y$|, %BW					
Forelimb	15.83 ± 7.46	13.44 ± 5.84	10.18 ± 7.73	11.44 ± 6.69	4.08 ± 2.28[*]
Hindlimb	15.18 ± 8.81	12.99 ± 6.22	9.55 ± 8.43	5.37 ± 6.25[*]	2.17 ± 2.24[*]
Area under GRF$_z$, %BW·s					
Forelimb	4.14 ± 0.81	4.53 ± 1.06	6.71 ± 1.17[*]	3.86 ± 1.42	2.30 ± 1.03[*]
Hindlimb	3.60 ± 1.09	4.07 ± 1.12	5.50 ± 1.86	1.29 ± 1.11[*]	1.91 ± 0.05[*]
GRF$_z$ onset, %BW/s					
Forelimb	2,239.86 ± 1,009.89	1,928.42 ± 572.65	565.32 ± 89.02[*]	566.54 ± 190.96[*]	318.98 ± 145.13[*]
Hindlimb	2,782.23 ± 1,185.03	2,323.04 ± 757.37[*]	600.89 ± 281.43[*]	210.48 ± 163.60[*]	192.28 ± 106.44[*]
Stance duration, s					
Forelimb	0.10 ± 0.02	0.14 ± 0.04[*]	0.30 ± 0.03[*]	0.33 ± 0.08[*]	0.26 ± 0.11[*]
Hindlimb	0.11 ± 0.01	0.13 ± 0.04	0.32 ± 0.05[*]	0.23 ± 0.12	0.37 ± 0.13[*]

Open in a new tab

Values are means ± SD; *n,* no. of mice. All measurements come from a single mouse, and footfalls were verified by video before analysis. GRF, ground reaction force; *x,* nose-to-tail; *y,* mediolateral; *z,* vertical; BW, body weight.

*Significantly different than Normal ($P < 0.05$).

Suspension also sharply reduced the rate of onset of vertical GRFs in both the forelimbs and the hindlimbs ([Table 1](#)). For example, with Mars suspension, the rate of vertical force onset was 73 and 92% lower than with full weight bearing in the forelimbs and hindlimbs, respectively. Stance duration was also significantly higher in suspended animals. Although the absolute magnitude of transverse GRFs (GRF_x and GRF_y) was lower in suspension, the ratio of each of these in-plane forces to vertical GRF_z tended to be larger, particularly in the hindlimb.

Body mass and food intake.

Following 2 days of adaptation to the forelimb jackets, there were no significant differences in initial body mass across the groups (mean = 20.5 ± 1.2 g). Food usage for Mars animals decreased sharply at the time of suspension, stabilizing between *days 6* and *7.* Consistent with this, Mars animals lost 6.5 ± 2.7% of their body mass during the first week ($P < 0.0001$ relative to Age controls, zz). In *weeks 2* and *3,* there were no significant differences in maintenance of body mass between Age and Mars groups, suggesting that stress levels had normalized.

Unexpected weight gain was seen in the jacketed control animals (Jacket), who experienced caloric restriction in the first week of the study, while being pair fed to match the Mars animals ([Fig. 3](#)). After an initial decline in both food consumption and body mass, the Jacket animals experienced a rapid increase in body mass, showing significantly higher weight gain in *weeks 2* and *3* (11 ± 5%) than Age or Mars animals (both 2 ± 1%, $P < 0.001$), resulting in a final Jacket body mass significantly higher than both Mars and Age controls ([Fig. 3](#)).

Fig. 3.
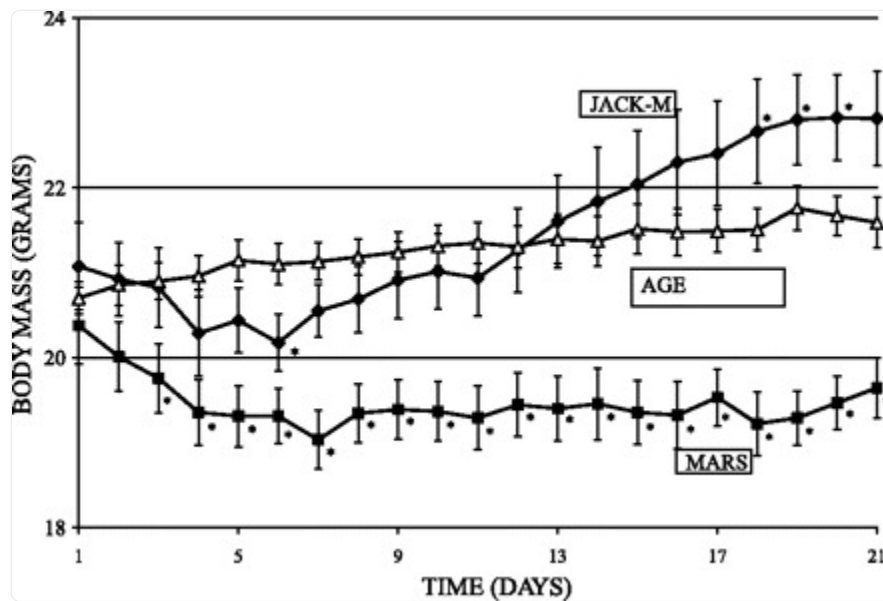
Daily body mass for 21-day Mars-analog suspension study in female mice. After an initial adaptation period, Mars animals (■) showed similar maintenance of weight as Age-matched controls (△). Jacket animals (♦) gained significantly more weight in the same period. Error bars represent ± SE. *Body mass significantly different from that of Age controls ($P < 0.05$).

Muscle mass.

Compared with Baseline values, Age animals had greater muscle mass. Mars animals had 20–23% lower gastrocnemius muscle wet mass than Jacket and Age controls (Table 2). Gastrocnemius mass normalized to body mass was also significantly lower for Mars animals relative to Age controls (−13%, $P = 0.04$). Despite their weight gain, Jacket animals did not show increased gastrocnemius wet mass compared with Age controls, either absolute or weight normalized.

Table 2.

Trabecular and cortical bone architecture and muscle mass following 21 days of Mars-analog loading in female mice

	Baseline	Age	Jacket	Mars
n	7–8	19–20	8	8–9
Trabecular bone architecture (distal femur)				
Bone volume fraction, %	23.51 ± 3.03	18.97 ± 2.60[c]	18.06 ± 1.60	14.34 ± 3.18[a,b]
Trabecular thickness, μm	54.97 ± 0.00	54.24 ± 2.30	53.26 ± 2.82	47.65 ± 1.85[a,b]
Trabecular number, mm^{-1}	5.24 ± 0.29	4.47 ± 0.30[c]	4.47 ± 0.18	4.37 ± 0.29
Trabecular spacing, μm	182.84 ± 12.34	217.84 ± 18.20[c]	216.65 ± 9.61	222.46 ± 15.06
Connectivity density, mm^{-3}	207.12 ± 23.89	137.35 ± 19.16[c]	145.84 ± 18.73	124.29 ± 26.29[b]
Structural model index	1.31 ± 0.30	1.62 ± 0.27[c]	1.79 ± 0.22	2.14 ± 0.40[a,b]
Cortical bone architecture (distal femur)[e]				
Cortical thickness, μm	166.57 ± 9.66	167.10 ± 8.06	158.60 ± 7.47[d]	134.00 ± 6.46[a,b]
Cortical bone architecture (femoral midshaft)				
Cross-sectional area, mm^2	1.55 ± 0.09	1.56 ± 0.09	1.55 ± 0.09	1.46 ± 0.10[a]
Cortical bone area, mm^2	0.87 ± 0.08	0.90 ± 0.05	0.87 ± 0.05	0.79 ± 0.05[a,b]
Minimum moment of inertia, mm^4	0.10 ± 0.01	0.11 ± 0.01	0.11 ± 0.01	0.09 ± 0.01[a,b]
Medullary area, mm^2	0.68 ± 0.08	0.66 ± 0.08	0.68 ± 0.07	0.68 ± 0.07
Cortical thickness, μm	223.75 ± 16.46	238.30 ± 13.47[c]	230.75 ± 5.31	212.44 ± 8.92[a,b]
Gastrocnemius muscle wet mass[f]				
Average mass, mg	107.88 ± 7.26	118.73 ± 5.58[c]	113.50 ± 9.19	90.88 ± 9.38[a,b]

	Baseline	Age	Jacket	Mars
Average mass/body mass, %	0.55 ± 0.02	0.55 ± 0.06	0.51 ± 0.01	0.48 ± 0.04[a]

Values are means ± SD; n, no. of mice ([e]$n = 10$ for Age; [f]$n = 8$ for Baseline, $n = 13$ for Age, $n = 2$ for Jacket, $n = 4$ for Mars).

[a]Mars significantly different than Age,

[b]Mars significantly different than Jacket,

[c]Age significantly different than Baseline, and

[d]Jacket significantly different from Age: $P < 0.05$.

Bone microarchitecture by μCT.

Compared with Baseline values, Age animals had decreased trabecular bone volume and a relative maintenance of cortical parameters (Table 2). Trabecular and cortical bone microarchitecture were further deteriorated in Mars animals compared with both Age and Jacket controls (Table 2). In the distal femoral metaphysis, trabecular BV/TV was 24% less in Mars than Age ($P = 0.0001$, Table 2), whereas there was no difference in trabecular number or separation. Rather, BV/TV losses were driven by a significant trabecular thinning, leading to a shift in the structural model index toward rodlike geometry.

At the femoral midshaft, Mars mice had a smaller cross-sectional area and area moments of inertia than Age controls (Table 2). Ct.Th and cortical BA at both the midshaft and the distal femoral metaphysis were also significantly lower in Mars than in Age controls. Similar results were seen for Mars animals relative to Jacket, with significantly smaller moments of inertia in the femoral midshaft, as well as reduced Ct.Th and BA in both the femoral midshaft and distal metaphysis.

Biomechanical properties.

In Mars mice, the morphometric changes described above were associated with significant decrements in biomechanical properties relative to Age-matched controls, as demonstrated by three-point bending to failure (Table 3). Failure (or ultimate) moment was 27% lower in Mars samples relative to Age controls ($P = 0.0002$). Bending stiffness and moment at yield were also significantly lower in Mars animals relative to Age controls ($P < 0.05$). When structural biomechanical properties were normalized to area moments of inertia, the resulting estimated Young's modulus did not

differ significantly between Mars and Age groups, suggesting that changes in biomechanical properties were due primarily to geometric changes.

Table 3.

Femoral biomechanical properties as determined by three-point bending following 21 days of Mars-analog loading in female mice

	Baseline	Age	Jacket	Mars
n	8	19	7–8	7–9
Stiffness, N/mm	125.85 ± 12.10	136.05 ± 10.13[‡]	113.76 ± 19.21[§]	114.70 ± 13.86[*]
Yield moment, N·mm	15.69 ± 5.56	17.33 ± 4.50	11.11 ± 4.39[§]	13.05 ± 1.21[*]
Ultimate moment, N·mm	26.10 ± 3.59	29.10 ± 3.90	22.94 ± 5.89[§]	21.20 ± 3.38[*]
Postyield bending work, N·mm	5.45 ± 2.16	5.51 ± 1.71	5.81 ± 1.86	5.67 ± 2.22
Estimated Young's modulus, N/mm^2	5,611.95 ± 598.13	5,584.61 ± 580.81	4,641.47 ± 580.42[§]	5,480.99 ± 702.87[†]

[Open in a new tab]

Values are means ± SD; *n*, no. of mice.
[*]Mars significantly different than Age,
[†]Mars significantly different than Jacket,
[‡]Age significantly different than Baseline, and
[§]Jacket significantly different than Age: $P < 0.05$.

Despite their similarities in morphology, the biomechanical properties of Jacket femurs were weaker than those of Age controls, and did not differ from those of Mars animals, with the exception of a lower estimated Young's modulus in Jacket specimens.

Histology.

Baseline animals had higher bone formation parameters than Age-controls (who were 3 wk older), including significantly increased mineral apposition rate, osteoid surface, and number of osteoblasts (Table 4). At the end of the study, compared with Age-matched controls, Mars animals had reduced indexes of bone formation, including significantly less mineralizing surface (per bone surface), and osteoid surface (per bone surface) (Table 4). Mars animals had lower osteoclast numbers compared with Age-matched controls. This observation, along with no differences in eroded surface, suggests unchanged or slightly lower rates of bone resorption in Mars animals. Jacket animals had significantly less mineralizing surface than Age controls, and more osteoclasts and osteoid surface than the Mars specimens.

Table 4.

Histological and histomorphometric data from the proximal tibia following 21 days of Mars-analog loading in female mice

	Baseline	Age	Jacket	Mars
n	5	5	5	5
MS/BS, %	18.58 ± 4.10	17.72 ± 6.80	10.62 ± 4.28§	11.19 ± 2.91*
BFR/BS, $\mu m^3 \cdot \mu m^{-2} \cdot yr^{-1}$	169.72 ± 62.13	105.50 ± 88.16	46.91 ± 44.55	43.38 ± 16.69
MAR, µm/day	2.49 ± 0.57	1.42 ± 0.63‡	1.03 ± 0.58	1.10 ± 0.23
OS/BS, %	3.19 ± 1.60	2.08 ± 0.29‡	2.09 ± 0.58	1.48 ± 0.42*†
ES/BS, %	1.10 ± 0.55	0.95 ± 0.20	1.12 ± 0.28	0.95 ± 0.18
O.Th, µm	6.78 ± 1.04	4.73 ± 0.60	3.73 ± 0.52	4.47 ± 1.48
N.Ob/BS, μm^{-1}	14.71 ± 4.72	7.29 ± 2.86‡	5.43 ± 0.11	6.00 ± 1.05
N.Oc/BS, μm^{-1}	0.48 ± 0.21	0.59 ± 0.07	0.63 ± 0.11	0.46 ± 0.17†

[Open in a new tab]

Values are means ± SD; n, no. of mice.
*Mars significantly different than Age ($P < 0.05$);
†Mars significantly different than Jacket ($P \leq 0.05$);
‡Age significantly different than Baseline ($P < 0.05$);
§Jacket significantly different than Age ($P < 0.05$).
MS, mineralized surface; BS, bone surface; BFR, bone formation rate; MAR, mineral apposition rate; OS, osteoid surface; ES, erosion surface; O.Th, osteoid thickness; N.Ob, number of osteoblasts; N.Oc, number of osteoclasts.

DISCUSSION

Our first objective was to develop a new rodent model of PWS to explore the musculoskeletal effects of chronically reduced weight bearing. In keeping with the key functional requirements outlined earlier, this study successfully

demonstrated extended quadrupedal partial weight bearing at tunable levels, while minimizing animal stress and adequately supporting characteristic animal behaviors. While not shown here, other studies by our group showed that mice removed from the PWS system after suspension were immediately able to return to full weight bearing.

More specifically, the design of our hardware and experimental methods ensured that average static loads were proportionally reduced relative to the degree of animal suspension. Daily weighing and titration of effective weight allowed for tight control of these chronic loads, generally to well within 5% of desired weight-bearing levels.

Force platform measurements of locomotor GRFs demonstrated that peak GRFs and force onset (i.e., strain rate) were lower for suspension animals than controls. The reductions in peak force were somewhat larger than predicted simply by the level of suspension, perhaps due to effects of dynamic locomotion and/or the independent effects of forelimb harnessing. Whereas jackets alone led to more equal weight sharing between the forelimbs and hindlimbs, suspension gaits tended to favor the forelimbs.

Observed increases in the ratio of transverse to vertical GRFs suggest a greater relative need for stabilization in partial weight-bearing animals, despite the moderating presence of harness forces. Such increased expenditure for postural stability is consistent with human studies of partial weight-bearing locomotion ([21]).

Some caution is warranted in interpreting gait data, as variable locomotor speeds were adopted under the different weight-bearing conditions. Across trials, suspended animals adopted a significantly lower average speed (10.98 ± 4.77 cm/s) than nonsuspended animals (38.69 ± 17.22 cm/s, $P < 0.0001$). Because peak force increases with decreasing stance time ([1]), it is, therefore, likely that our data underestimate the amount of peak force reduction that might be observed in a speed-matched trial. A variety of changes in gait kinematics and dynamics have been seen in prior studies of human partial weight bearing and may well be expected under true partial gravity conditions ([21], [22]). Like these studies, our data do not show linear reductions in peak vertical GRFs during walking, but they are representative of free gait for each of our experimental conditions and should be characteristic of the actual peak forces observed during daily living for each group. Additionally, all locomotor data were acquired in an animal newly adapted to suspension. Future studies should investigate whether there are additional differences associated with neuromuscular adaptation or disuse-induced muscle loss following chronic exposure to partial weight bearing.

Our second objective was to use our partial weight-bearing system to conduct the first study of adaptation to Mars gravity levels. We found that 3 wk of Mars analog loading was well tolerated and led to significant musculoskeletal deterioration relative to age-matched controls.

We utilized 10-wk-old BALB/cByJ female mice, as this is an age when longitudinal growth and body mass gains are minimal. Moreover, at this age, trabecular bone volume is at near maximal levels ([5], [6]), which mimics peak bone mass of most astronauts and which optimized our ability to detect declines in trabecular bone. Compared with the Baseline

group, normally weight-bearing Age controls had decreased trabecular bone volume, but increased cortical thickness at the femoral diaphysis, which was accompanied by significant increases in stiffness. Additional studies are needed to determine whether age influences the musculoskeletal adaptation to partial weight bearing, as has been suggested for hindlimb suspension ([27]).

Corticosterone and other systemic stress hormones are known to be catabolic to both muscle and bone. In tail-suspension studies, body mass has been established as a gross surrogate marker for chronic systemic stress ([17]). The weight loss in the Mars-analog and jacketed control animals during the first week of suspension suggests a brief period of increased stress and adaptation to the experimental environment, due to some combination of environmental or feeding effects, not simply suspension. However, the return of normal growth rates in Mars animals in *weeks 2* and *3*, and the accompanying stabilization of food consumption, suggest that systemic stress due to the experimental treatment is negligible after the initial adaptive period. Similar results have been seen in centrifuge studies ([30], [31]) and tail-suspension experiments ([32]). In future PWS studies, characterization of corticosterone levels could provide a more sensitive stress profile. Additional cohorts killed during the study for histomorphometry could also clarify if this transient is associated with changes in bone resorption, which may be obscured in our poststudy measures.

As noted, jacketed but fully weight-bearing mice experienced an unexpected increase in body mass, showing significantly higher weight gain in the second and third weeks of the study compared with either age-matched or Mars-analog animals. This weight gain was not correlated with additional longitudinal bone growth or muscle gain in the gastrocnemius, suggesting a shift in body composition toward higher fat content or muscular hypertrophy elsewhere in the body.

Caloric restriction in mice results in significantly decreased resting metabolic rate and reductions in energy expenditures from exercise ([7]). Weight gain in calorically restricted animals is largely due to increases in adipose body fraction, while lean mass changes are curtailed relative to controls. If the pair-fed jacketed animals adopted a reduced metabolic rate during caloric restriction, then returned to normal consumption levels, weight gain and increasing body fat may have been expected. Future studies should incorporate longitudinal measures of body composition to resolve this open question. Additionally, activity levels may vary between groups and should be monitored in future studies to better differentiate the impact of this variable on key outcomes.

Due to the sharp body mass increase in Jacket controls and the strong relationship between musculoskeletal parameters and body mass ([3]), we focused our analysis on the comparison between Mars and Age animals, which had similar body weights. Patterns of bone loss were generally consistent with previous reports from tail-suspension experiments, with greater losses in the trabecular compartment than cortical, and sharper reductions in bone formation than resorption, as observed at the end of the study.

While we believe the predominant effects of PWS are due to differences in weight bearing, a few observations (i.e.,

femoral biomechanics and tibial histology) taken at the end of the experiment showing differences between jacketed, fully weight-bearing mice and age-matched controls suggest that the musculoskeletal response may have been influenced by the experimental conditions themselves. There are several factors that may have contributed to these observations. First, Jacket mice were singly housed, whereas Age-matched controls were group housed. This is relevant, as singly housed mice have been shown to have lower whole body bone mass relative to group-housed mice ([20]). Second, jacketed mice were pair fed to Mars consumption levels and thus calorie restricted relative to age-matched controls. Finally, jacketed mice were restrained slightly by the jacket and exhibited altered gait compared with unjacketed controls. Altogether, these factors may have contributed to the differences between age-matched and jacketed animals. Further studies with additional control groups (i.e., singly housed, no jacket), larger group sizes, and alternate time points are needed to delineate the effects of weight-bearing status vs. experimental conditions.

Mice exposed to partial weight bearing exhibited several physiological changes consistent with those previously reported in hindlimb suspension studies, including decreased muscle and bone mass and reduced bone formation indexes. Compared with a previously published study of hindlimb suspension in female mice of the same genetic background, both cortical and trabecular bone losses in Mars animals were less than those previously reported for this mouse strain ([9]). However, we note that this observation was made by comparing studies conducted in different laboratories, and, although provocative, it is clear that additional studies are needed to provide direct comparisons of the musculoskeletal adaptations to various partial weight-bearing and full unloading environments. In particular, the addition of a tail-suspension control to future studies of partial weight bearing will enable researchers to better explore the potentially osteoprotective effects of partial weight bearing in contrast to full unloading and the role of fluid shift in these changes.

Our model of reduced gravitational loading is subject to many of the limitations common to all ground-based models of partial weight bearing. In particular, suspension forces are localized at the harness points, while normal Earth gravity acts on the distributed masses of the limbs. Suspension hardware somewhat limits the animals' range of motion, particularly in the spine, and is not tolerated well by all animals. Experience in harnessing and suspending is necessary to minimize morbidity.

There is some variation of upward force across the gait cycle due to small displacements of the animal's center of mass during normal locomotion. Furthermore, sensorimotor changes expected in true reduced-gravity environments due to altered vestibular inputs are not present. However, our data indicate that the PWS system is able to model chronic conditions of reduced dynamic loading of the musculoskeletal system, providing a valuable tool for investigations in this area. Selection of an appropriate control depends on experimental objectives, but should account for the effects of single housing in novel cage structures without bedding. Data presented here suggest that application of a forelimb jacket in fully weight-bearing animals may have side effects of increased weight gain and alterations in gait. Further study is required to understand the origin and impacts of these changes.

Traditional tail suspension studies utilize a 30° head-down suspension to provide normal loads to the forelimbs without excessive tension on the tail ([8]). However, while notable cephalic fluid shift and the diuresis it engenders are typical of human flight responses, the magnitude is excessive relative to actual flight responses in small quadrupeds ([28]). Thus our model, which does not cause fluid shift, may, in fact, more accurately represent rodent spaceflight changes.

In conclusion, we have presented a novel approach to ground studies of chronic partial weight bearing that is extensible to a wide range of loading regimes, including studies of interventions and reloading. Three weeks of Mars-analog loading showed decreased muscle mass, along with deterioration of both cortical and trabecular bone relative to controls. Further studies are needed to explore whether there is a threshold of loading beyond which such skeletal degradation slows appreciably, offering key insights into countermeasures against bone loss in spaceflight, bed rest, and other catabolic states. Such studies would have direct relevance for human spaceflight, as well as clinical conditions of reduced musculoskeletal loading due to disease, injury, or inactivity.

GRANTS

DISCLOSURES

ACKNOWLEDGMENTS

REFERENCES

1. Clarke KA, Smart L, Still J. Ground reaction force and spatiotemporal measurements of the gait of the

mouse. Behav Res Methods Instrum Comput 33: 422–426, 2001 [DOI   ] [PubMed] [Google Scholar   ]

2. Davis BL, Cavanagh PR. Simulating reduced gravity: a review of biomechanical issues pertaining to human locomotion. Aviat Space Environ Med 64: 557–566, 1993 [PubMed] [Google Scholar   ]

3. Felson DT, Zhang Y, Hannan MT, Anderson JJ. Effects of weight and body mass index on bone mineral density in men and women: the Framingham study. J Bone Miner Res 8: 567–573, 1993 [DOI   ] [PubMed] [Google Scholar   ]

4. Frost HM. Bone "mass" and the "mechanostat": a proposal. Anat Rec 219: 1–9, 1987 [DOI   ] [PubMed] [Google Scholar   ]

5. Glatt V, Canalis E, Stadmeyer L, Bouxsein ML. Age-related changes in trabecular architecture differ in female and male C57BL/6J mice. J Bone Miner Res 22: 1197–1207, 2007a [DOI   ] [PubMed] [Google Scholar   ]

6. Glatt V, Shultz KL, Beamer WG, Rosen CJ, Bouxsein ML. Age-related changes in bone architecture vary among inbred strains of mice. Bone 40: S194, 2007 [Google Scholar   ]

7. Hambly C, Speakman JR. Contribution of different mechanisms to compensation for energy restriction in the mouse. Obes Res 13: 1548–1557, 2005 [DOI   ] [PubMed] [Google Scholar   ]

8. Hargens AR, Steskal J, Johansson C, Tipton CM. Tissue fluid shift, forelimb loading, and tail tension in tail-suspended rats. Physiologist 27: S37–S38, 1984 [Google Scholar   ]

9. Judex S, Garman R, Squire M, Busa B, Donahue LR, Rubin C. Genetically linked site-specificity of disuse osteoporosis. J Bone Miner Res 19: 607–613, 2004 [DOI   ] [PubMed] [Google Scholar   ]

10. Judex S, Gross TS, Zernicke RF. Strain gradients correlate with sites of exercise-induced bone-forming surfaces in the adult skeleton. J Bone Miner Res 12: 1737–1745, 1997 [DOI   ] [PubMed] [Google Scholar   ]

11. Keyak JH, Koyama AK, Leblanc A, Lu Y, Lang TF. Reduction in proximal femoral strength due to long-duration spaceflight. Bone 44: 449–453, 2009 [DOI   ] [PubMed] [Google Scholar   ]

12. Lang T, LeBlanc A, Evans H, Lu Y, Genant H, Yu A. Cortical and trabecular bone mineral loss from the spine and hip in long-duration spaceflight. J Bone Miner Res 19: 1006–1012, 2004 [DOI   ] [PubMed] [Google Scholar   ]

13. Lang TF. Skeletal atrophy and long-term recovery in long-duration spaceflight. In: 16th Humans in Space Symposium of the International Academy of Astronautics, Beijing, China, 2007 [Google Scholar   ]

14. Lang TF, Leblanc AD, Evans HJ, Lu Y. Adaptation of the proximal femur to skeletal reloading after long-

duration spaceflight. J Bone Miner Res 21: 1224–1230, 2006 [DOI] [PubMed] [Google Scholar]

15. LeBlanc A, Schneider V, Shackelford L, West S, Oganov V, Bakulin A, Voronin L. Bone mineral and lean tissue loss after long duration space flight. J Musculoskelet Neuronal Interact 1: 157–160, 2000 [PubMed] [Google Scholar]

16. Looker AC, Wahner HW, Dunn WL, Calvo MS, Harris TB, Heyse SP, Johnston CC, Jr, Lindsay R. Updated data on proximal femur bone mineral levels of US adults. Osteoporos Int 8: 468–489, 1998 [DOI] [PubMed] [Google Scholar]

17. Morey-Holton ER, Globus RK. Hindlimb unloading of growing rats: a model for predicting skeletal changes during space flight. Bone 22: 83S–88S, 1998 [DOI] [PubMed] [Google Scholar]

18. Morey-Holton ER, Globus RK. Hindlimb unloading rodent model: technical aspects. J Appl Physiol 92: 1367–1377, 2002 [DOI] [PubMed] [Google Scholar]

19. Musacchia XJ, Deavers DR. A new rat model for studies of hypokinesia and antiorthostasis. Physiologist 23: S91–S92, 1980 [PubMed] [Google Scholar]

20. Nagy TR, Krzywanski D, Li J, Meleth S, Desmond R. Effect of group vs. single housing on phenotypic variance in C57BL/6J mice. Obes Res 10: 412–415, 2002 [DOI] [PubMed] [Google Scholar]

21. Newman DJ, Alexander HL. Human locomotion and workload for simulated lunar and Martian environments. Acta Astronaut 29: 613–620, 1993 [DOI] [PubMed] [Google Scholar]

22. Newman DJ, Alexander HL, Webbon BW. Energetics and mechanics for partial gravity locomotion. Aviat Space Environ Med 65: 815–823, 1994 [PubMed] [Google Scholar]

23. Parfitt AM, Drezner MK, Glorieux FH, Kanis JA, Malluche H, Meunier PJ, Ott SM, Recker RR. Bone histomorphometry: standardization of nomenclature, symbols, and units. Report of the ASBMR Histomorphometry Nomenclature Committee. J Bone Miner Res 2: 595–610, 1987 [DOI] [PubMed] [Google Scholar]

24. Rubin CT, Lanyon LE. Kappa Delta Award paper. Osteoregulatory nature of mechanical stimuli: function as a determinant for adaptive remodeling in bone. J Orthop Res 5: 300–310, 1987 [DOI] [PubMed] [Google Scholar]

25. Schultheis L, Ruff CB, Rastogi S, Bloomfield S, Hogan HA, Fedarko N, Thierry-Palmer M, Ruiz J, Bauss F, Shapiro JR. Disuse bone loss in hindquarter suspended rats: partial weightbearing, exercise and ibandronate treatment as countermeasures. J Gravit Physiol 7: P13–P14, 2000 [PubMed] [Google Scholar]

26. Sims NA, Clement-Lacroix P, Minet D, Fraslon-Vanhulle C, Gaillard-Kelly M, Resche-Rigon M, Baron

R. A functional androgen receptor is not sufficient to allow estradiol to protect bone after gonadectomy in estradiol receptor-deficient mice. J Clin Invest 111: 1319–1327, 2003 [DOI] [PMC free article] [PubMed] [Google Scholar]

27. Simske SJ, Luttges MW, Wachtel H. Age dependent development of osteopenia in the long bones of tail-suspended mice. Biomed Sci Instrum 26: 87–94, 1990 [PubMed] [Google Scholar]

28. Tanaka K, Gotoh TM, Awazu C, Morita H. Regional difference of blood flow in anesthetized rats during reduced gravity induced by parabolic flight. J Appl Physiol 99: 2144–2148, 2005 [DOI] [PubMed] [Google Scholar]

29. Turner RT. Invited review: what do we know about the effects of spaceflight on bone? J Appl Physiol 89: 840–847, 2000 [DOI] [PubMed] [Google Scholar]

30. Wade CE, Harper JS, Daunton NG, Corcoran ML, Morey-Holton E. Body mass change during altered gravity: spaceflight, centrifugation, and return to 1 G. J Gravit Physiol 4: 43–48, 1997 [PubMed] [Google Scholar]

31. Warren LE, Horwitz BA, Hamilton JS, Fuller CA. Effects of 2 G on adiposity, leptin, lipoprotein lipase, and uncoupling protein-1 in lean and obese Zucker rats. J Appl Physiol 90: 606–614, 2001 [DOI] [PubMed] [Google Scholar]

32. Wronski TJ, Morey-Holton ER. Skeletal response to simulated weightlessness: a comparison of suspension techniques. Aviat Space Environ Med 58: 63–68, 1987 [PubMed] [Google Scholar]

33. Zumwalt AC, Hamrick M, Schmitt D. Force plate for measuring the ground reaction forces in small animal locomotion. J Biomech 39: 2877–2881, 2006 [DOI] [PubMed] [Google Scholar]